기초강좌

Application of Piezoelectric-based Actuators to Helicopter Vibration Reduction (4)

Jun-Sik Kim*
(Assistant Professor of Mechanical Engineering Kumoh Nat'l Institute of Technology)

Many methodologies have been explored to reduce helicopter vibration. Trailing edge flaps for such a purpose have been studied for the past twenty years. A brief overview of the introduction of active vibration controls using trailing edge flaps and smart actuators is presented in series. This is the fourth article, in which a piezoelectric resonant actuation system with a buckling-beam motion amplifier for active trailing edge flaps is presented.

1. Introduction

Piezoelectric material based actuators have shown good potential for various applications, such as trailing-edge flaps for rotary-wing vehicles. These piezoelectric actuators are compact, high force and high bandwidth devices, but can only provide a limited stroke. This limitation can be critical in cases where large trailing-edge flap deflections or large size rotor blades are needed. Efforts to improve the piezoelectric actuator performance have been carried out by researchers in developing amplification mechanisms of various types.

To advance the state of the art and further enhance the authority of piezoelectric material-based actuation systems, various new ideas have been explored in recent years. A novel motion amplifier has been developed by Jiang and Mockensturm to increase the output work transferred through a compliant structure. The concept is to induce elastic and dynamic instability of an axially driven buckling beam to amplify the actuator motion. Another innovative idea is to achieve a high-authority piezoelectric resonant actuation system via mechanical and electrical tailoring.

From reviewing the current buckling beam motion amplifier and resonant actuator concepts, it is

* E-mail : junsik.kim@kumoh.ac.kr / Tel : (054) 478-7397

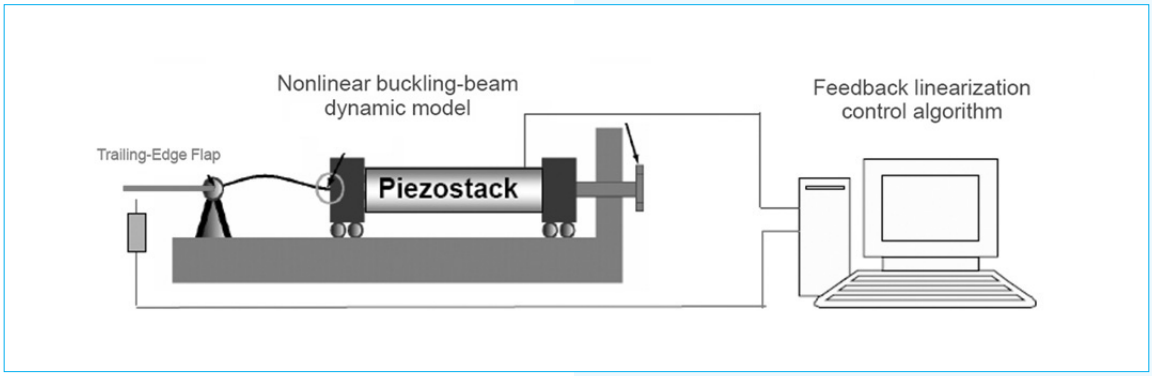

Fig. 1 A buckling beam motion amplifier with a feedback linearization control

recognized that an approach that combine the two ideas could further advance the state of the art in achieving high authority, light weight and compact piezoelectric actuators. In other words, the aim here is to seek solutions that can effectively tailor and control the piezoelectric/buckling beam motion amplifier element to operate as a resonant actuation system (Fig. 1). In this case, resonance means that the operating frequency is at or near the natural frequency of the linearized system, which will cause significant amplification effect of the nonlinear motion amplifier.

2. System Description

A buckling beam actuator is illustrated in Fig. 2, where the hinged-clamped beam is attached to a piezoelectric stack actuator. The beam has an initial geometric imperfection, w^0, and it is under the axial static and dynamic loading, $P(t) = P_s + P_t \cos(\omega t)$ that is produced by both the preloading and the piezoelectric stack actuator, at the clamped end.

Assuming that the beam is a homogeneous one-dimensional elastic body, the total potential energy, which includes the strain energy due to bending and the potential energy of the applied axial load $P(t)$ at $x = l$, is expressed as:

$$\pi = \frac{1}{2} EI \int_0^l (\kappa - \kappa_o)^2 dx + \hat{P}(t) \int_0^l \hat{u}_{,x} dx \tag{1}$$

where E is the Young's modulus, and I is the moment of inertia of the cross-section of the beam.

By taking into account Eq. (1), neglecting rotary inertia and axial dynamics, and applying the ordering scheme, one can derive the following equation.

$$\begin{aligned} &\ddot{w} + c\dot{w} + w''''(w')^2 + 4w'''w''w' + (w'')^3 + w'''' \\ &+ P_s\left\{w^{o\prime\prime} + w'' + \frac{3}{2}w''(w')^2\right\} \\ &+ P_t\left\{w^{o\prime\prime} + w'' + \frac{3}{2}w''(w')^2\right\}\cos\Omega\tau = 0 \end{aligned} \tag{2}$$

where the superscript 'o' indicates the initial imperfection, the overdot represents the derivative with respect to the nondimensionalized time, τ, and the prime denotes the derivative with respect to the normalized spatial coordinate, ξ. The corresponding

기초강좌

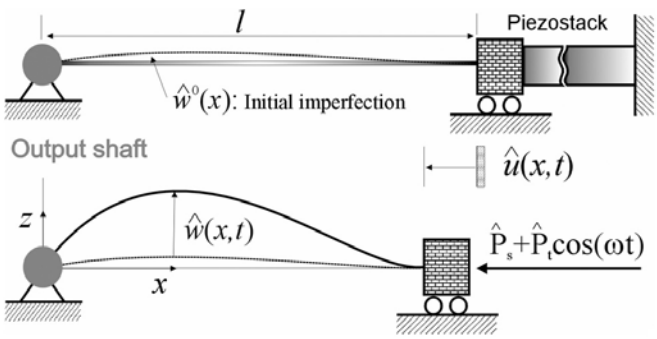

Fig. 2 Schematic of the piezoelectric buckling beam actuation system

boundary conditions are read as:

$$\begin{aligned} &w=0 \ \text{ and } \ w''\left\{1+(w')^2\right\}=0 \ \ at \ \ \xi=0 \\ &w=0 \ \text{ and } \ w'=0 \ \ at \ \ \xi=1 \end{aligned} \tag{3}$$

The post-buckling behavior of the beam needs to be analyzed in order to characterize the beam dynamics around the static equilibrium. The governing equation of the buckling problem can be obtained from Eq. (2) by dropping the time derivatives and the dynamic axial load, and the boundary conditions from Eq. (3). The Galerkin method is then adopted to solve the nonlinear buckling equation. It is assumed that the geometric imperfection is given by the same buckling mode shape. To obtain the governing equations of beam dynamics around the static equilibrium, we let the transverse displacement be

$$w(\xi,\tau)=w_s(\xi)+v(\xi,\tau) \tag{4}$$

where $w_s(\xi)$ is the statically deformed configuration corresponding to the static compressive load P_s. $v(\xi,\tau)$ denotes a time-dependent perturbation around the deformed and/or buckled configuration.

Substituting Eq. (4) into Eq. (2) yields the nonlinear dynamic equation

$$\begin{aligned} &\ddot{v}+c\dot{v}+\mathcal{L}_3(v)+P\mathcal{G}_3(v)+\mathcal{L}_2(v)+P\mathcal{G}_2(v) \\ &\quad +\mathcal{L}_1(v)+P\mathcal{G}_1(v)=-P_t\ \mathcal{G}_o\cos(\Omega\tau) \end{aligned} \tag{5}$$

where $P=P_s+P_t\cos(\Omega\tau)$, $\mathcal{L}_i(v)$ and $\mathcal{G}_i(v)$ are differential operators. Equation (5) forms a nonlinear Mathieu-type equation. The Galerkin method is again employed to discretize the nonlinear equations of motion. Subsequently a single mode approximation is applied to the system equation, and the modal equation is then summarized as follows:

$$\begin{aligned} &\ddot{q}+2\mu\Omega_s\dot{q}+(\Omega_s^2+P_t f_1\cos\Omega\tau)q+(\alpha_2+P_t f_2\cos\Omega\tau)q^2 \\ &\quad +(\alpha_3+P_t f_3\cos\Omega\tau)q^3=-P_t f_e\cos\Omega\tau \end{aligned} \tag{6}$$

where Ω_s denotes the first natural frequency. Calculations of the modal damping ratio, μ, parametric excitation magnitude f_i, and external

excitation magnitude f_e are straightforward.

It should be noted here that a single-mode descretization could yield quantitatively as well as qualitatively erroneous static and dynamic responses for relatively high buckling levels ($b_s > 1$). In this article, however, we are interested in the vicinity of the first critical buckling load, where $b_s << 1$. Thus a single-mode descretization gives us a good approximation, especially when initial imperfections are considered. Henceforth, a Mathieu-type nonlinear dynamic model derived herein, Eq. (6), will be used to analyze the nonlinear dynamic behavior of the post-buckled beam under axial dynamic loads.

3. Output Feedback Linearization Control Algorithm

To obtain the desired output of the beam (the rotation angle at the hinged end, $\xi = 0$) at the operating frequency, the piezoelectric stack actuator needs to be effectively controlled. The post-buckled beam dynamics together with feedback linearization control algorithm based on a "high-gain estimator" can be used for such purpose.

It is assumed that the piezoelectric actuator dynamics is negligible since its natural frequency is much higher than that of the post-buckled beam, so that the actuation voltage is linearly proportional to the axial dynamic load.

One can obtain a corresponding state-space form of Eq. (6) as:

$$\begin{aligned} \dot{x}_1 &= x_2 \\ \dot{x}_2 &= \Theta(x_1, x_2, \tau) + \beta(x_1) u_C \end{aligned} \tag{7}$$

where Θ is the nonlinear function including the damping and forcing terms, u_C is the axial dynamic control load, and β represents the nonlinear geometric shape of the post-buckled beam.

In general, the nonlinear function $\Theta(x_1, x_2, \tau)$ has significant uncertainties. It, therefore, cannot be directly used in a controller design. These uncertainties can be lumped into a new state η and treat it as unknown. Then Eq. (7) becomes

$$\begin{aligned} \dot{x}_1 &= x_2 \\ \dot{x}_2 &= \eta + \beta(x_1) u_C \\ \dot{\eta} &= \Xi(x_1, x_2, \eta, u_C, \tau) \end{aligned} \tag{8}$$

where

$$\Xi(x_1, x_2, \eta, u_C, \tau) = \sum_{i=1}^{2} \frac{\partial \Theta}{\partial x_i} \frac{\partial x_i}{\partial \tau} + \frac{\partial \Theta}{\partial \tau} \tag{9}$$

The control law for a feedback linearization based on estimated state variables is now read as:

$$u_C = \left(\dot{x}_{2d} - \tilde{\eta} + \tilde{\mathbf{K}} \tilde{\mathbf{e}} \right) / \tilde{\beta} \tag{10}$$

where

$$\tilde{\mathbf{e}} = \begin{bmatrix} \tilde{x}_1 - x_{1d} & \tilde{x}_2 - x_{2d} \end{bmatrix}^T, \quad \mathrm{sgn}(\tilde{\beta}) = \mathrm{sgn}(\beta) \tag{11}$$

Here it is assumed that an estimation of β is available from feedback (i.e., x_1 state variable), so that it can be compensated by the control u_C even if there are modeling errors in geometric stiffness terms such as f_1, f_2, f_3 and f_e.

Now one can use the feedback control law, Eq. (10), to suppress the undesirable nonlinear dynamic behaviors. It should be noted here that the large feedback control input to the nonlinear dynamic

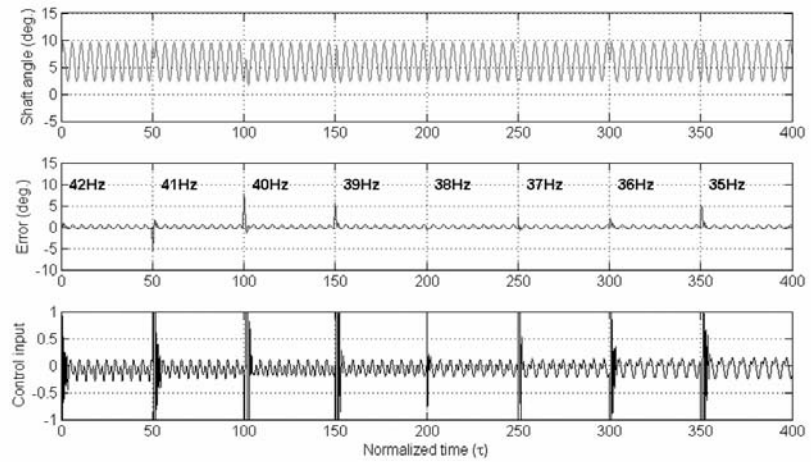

Fig. 3 Time response of controlled system, error from desired shaft angle, and control input with frequency sweep down

system can induce the so-called peaking phenomenon, especially when high-gain observers are employed. This leads to system instabilities. In addition to these instabilities, the current dynamic system includes parametric excitations, and the feedback control input contributes to these excitations via the nonlinear geometric stiffness, β. To eliminate these effects, the feedback control law is modified by a saturation function of $sat(u_C)$ which is defined as follows:

$$u_C^m = sat(u_C) = \begin{cases} u_C & \text{if } |u_C| \le U_{\max} \\ \text{sgn}(u_C) U_{\max} & \text{if } |u_C| > U_{\max} \end{cases} \quad (12)$$

4. Concluding Remarks

The time response of a controlled system, the deviation from the desired shaft angles and the control signal are presented in Fig. 3. One can see that shaft angles of 2 to 10 degrees are achieved throughout the time period. Notice here that shaft angles are shifted from ±4 degrees to 2~10 degrees due to the static shaft angle (6 degrees) induced from the static compressive load P_s. As shown in Figure 8, the high authority resonant actuation can be achieved by the feedback linearization control based on a high-gain estimator for a piezoelectric buckling-beam motion amplifier. KSNVE

「기획 : 김흥수 편집위원 heungsoo@dongguk.edu」